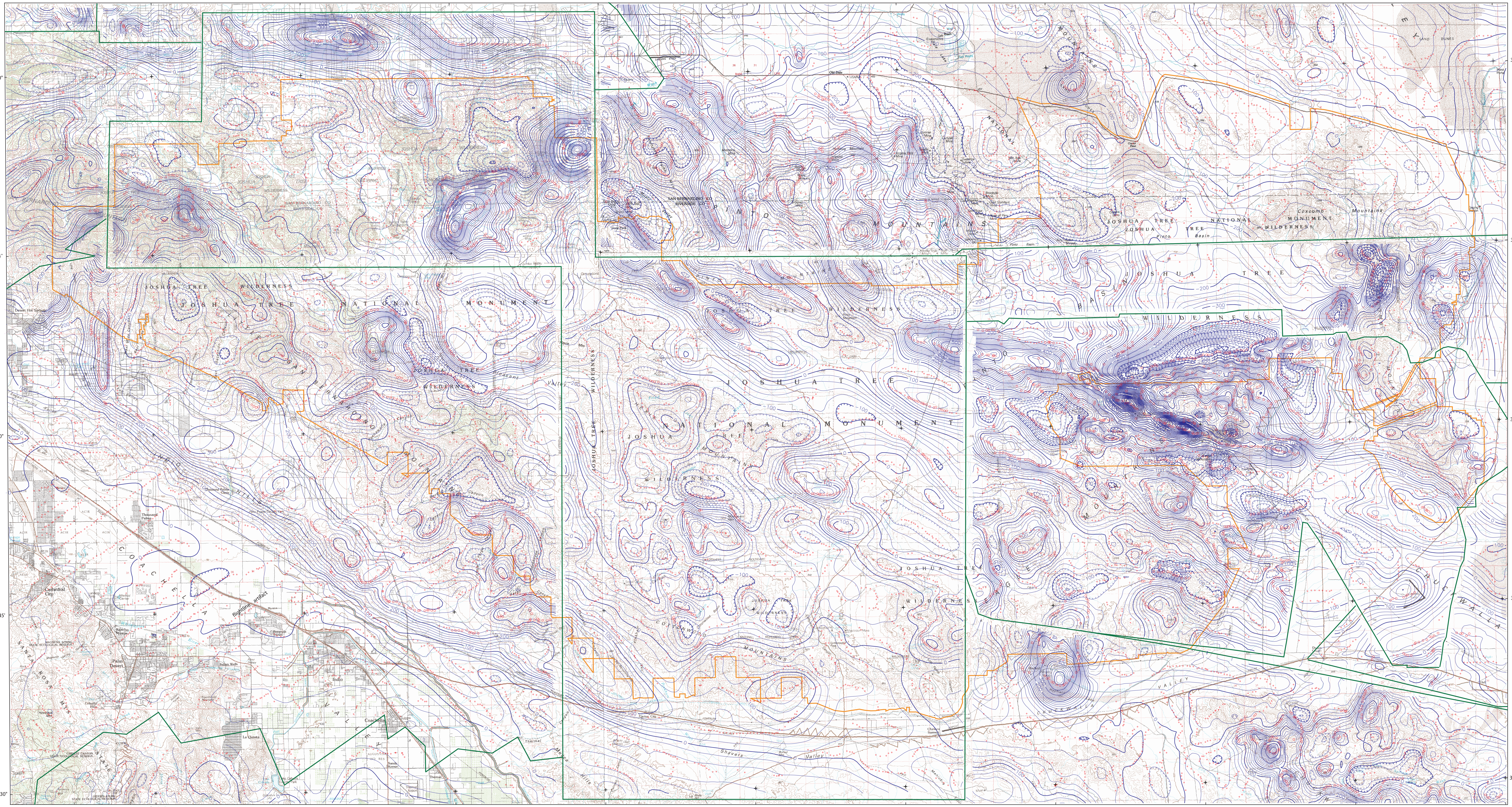

Topographic base from U.S. Geological Survey Palm Springs, Big Bear Lake, Sheephole Mountains, and Eagle Mountains 1:100,000-scale quadrangles.

SCALE 1:100,000

Manuscript approved for publication March 31, 2010

Preliminary Aeromagnetic Map of Joshua Tree National Park and Vicinity, Southern California

By

V.E. Langenheim and P.L. Hill

2010

Index Map

MAP EXPLANATION

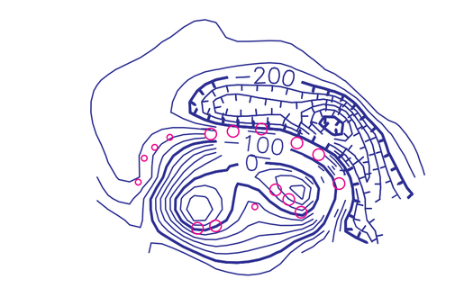

Contours of total magnetic field intensity relative to the International Geomagnetic Reference Field. Contour interval is 20 nanoteslas. Hachures indicate closed magnetic lows.

Joshua Tree National Park boundary, locally generalized for cartographic display

Aeromagnetic survey boundary

Location of maximum horizontal gradient, with amplitudes greater than the mean for the study area

Location of maximum horizontal gradient, with amplitudes less than the mean for the study area

DISCUSSION

This aeromagnetic map of Joshua Tree National Park and vicinity is intended to promote further understanding of the geology and structure in the region by serving as a basis for geophysical interpretations and by supporting geological mapping, water-resource investigations, and various topical studies. Local spatial variations in the Earth's magnetic field (evident as anomalies on aeromagnetic maps) reflect the distribution of magnetic minerals, primarily magnetite, in the underlying rocks. In many cases the volume content of magnetic minerals can be related to rock type, and abrupt spatial changes in the amount of magnetic minerals commonly mark lithologic or structural boundaries. Bodies of mafic and ultramafic rocks tend to produce the most intense magnetic anomalies, but such generalizations must be applied with caution because rocks with more felsic compositions, or even some sedimentary units, also can cause measurable magnetic anomalies.

Total-field aeromagnetic data from multiple surveys (table 1, index map) were used to construct the aeromagnetic map of Joshua Tree National Park and vicinity. All surveys, except for one, have been published previously. To eliminate poor coverage of the western Joshua Tree National Park, total-field aeromagnetic data were collected in September 2008 along north-south flight lines spaced 800 m apart and at a nominal terrain clearance of 305 m (table 1, Fig. 1, Joshua Tree survey). East-west tie lines were flown 8,000 m apart. Data were adjusted for tail-sensor lag and diurnal field variations. Further processing included micro-leveling using the tielines and subtraction of the reference field defined by IGRF2005 extrapolated to August 1, 2008.

Data from all the surveys were transformed to a Universal Transverse Mercator Projection (Base Latitude 0°, Central Meridian -117° W.) and interpolated to a square grid with a grid interval of 250 m using the principle of minimum curvature (Briggs, 1974). The magnetic base levels of the surveys were then adjusted to bring them onto a common magnetic datum; a 1-km wide gap separates the various surveys.

The red circles on the map (brown dots on fig. 2) indicate possible locations of abrupt lateral changes in magnetization and may represent lithologic or structural boundaries, although note that the northeast-trending alignments of circles in the southwest corner of the map are flightline artifacts. Their locations were determined as follows:

(1) The total-field magnetic anomaly data were mathematically transformed into pseudogravity anomalies (Baranov, 1957); this procedure effectively converts the magnetic field to the "gravity" field that would be produced if all the magnetic material were replaced by proportionately dense material.

(2) The pseudogravity field was continued upward a distance of 100 m and subtracted from the original pseudogravity field. This procedure emphasizes those components of the pseudogravity field that are caused by the shallow parts of the magnetic bodies, which are most closely related to the mapped geology.

(3) The horizontal gradient of the pseudogravity field difference was calculated everywhere by numerical differentiation.

(4) Locations of locally steepest horizontal gradient (circles) were determined by numerically searching for maxima in the horizontal gradient grid (Blakely and Simpson, 1986).

Boundaries between bodies having different densities are characterized by steep gradients in the gravity field they produce and, if the boundaries have moderate-to-steep dips (greater than 45°), locally the maximum horizontal gradients will be located over the surface traces of the boundaries (Blakely and Simpson, 1986). Similarly, boundaries between bodies having different magnetizations are characterized by steep gradients in the pseudogravity field and, therefore, the procedure described above can be used to locate these boundaries. For example, the circles coincide locally with strands of the Pinto Mountain, Blue Cut and Chiriaco Faults and can be used to map bedrock fault strands concealed by young deposits, such as shown by Langenheim and Powell (2009).

REFERENCES CITED

Baranov, V.I., 1957, A new method for interpretation of aeromagnetic maps—Pseudo-gravimetric anomalies: Geophysics, v. 22, p. 359-383.

Blakely, R.J., and Simpson, R.W., 1986, Approximating edges of source bodies from magnetic or gravity anomalies: Geophysics, v. 51, p. 1494-1498.

Briggs, I.C., 1974, Machine contouring using minimum curvature: Geophysics, v. 39, p. 39-48.

Grauch, V.J.S., 1984, Aeromagnetic map of the Eagle Mountains area, Riverside County, California: U.S. Geological Survey Open-File Report 84-502, scale 1:62,500.

Langenheim, V.E., and Powell, R.E., 2009, Basin geometry and cumulative offsets in the Eastern Transverse Ranges, southern California: Implications for transrotational deformation along the San Andreas fault system: Geosphere, v. 5, no. 1, p. 1-22.

LK&B Resources, Inc., 1980, NURE aerial gamma-ray and magnetic reconnaissance survey, Colorado-Arizona area, Salton Sea NI 11-9, El Centro NI11-12, Phoenix NI 12-7, Ajo NI12-10, and Lukeville NH 12-1, quadrangles: U.S. Department of Energy, Grand Junction Office Report GJBX-012(80), 5 vols.

Sweeney, R.E., 2002, Six aeromagnetic surveys in California, Nevada, and Arizona: A web site for distribution of data: U.S. Geological Survey Open-File Report 02-486 (http:// pubs.usgs.gov/of/2002/ofr-02-486).

U.S. Geological Survey, 1981, Aeromagnetic map of the Needles 1° by 2° quadrangle, California and Arizona: U.S. Geological Survey Open-File Report 81-085, scale 1:250,000.

U.S. Geological Survey, 1983, Aeromagnetic map of the Salton Sea area, California: U.S. Geological Survey Open-File Report 83-664, scale 1:250,000.

U.S. Geological Survey, 1985, Aeromagnetic map of the Palen area, Riverside County, California: U.S. Geological Survey Open-File Report 85-281, scale 1:62,500.

U.S. Geological Survey, 1990, Aeromagnetic map of parts of the San Diego, Santa Ana, and adjacent 1° by 2° quadrangles, California: U.S. Geological

Table 1. Surveys used to create aeromagnetic map

Survey	Year Flown	Flight elevation above ground	Flightline spacing	Flightline direction	Reference
Eagle Mountains	1954	Variable	Variable	Variable	Grauch (1984)
NURE	1978	122 m	4800 m	N-S	LK&B Resources, Inc. (1980)
Needles	1980	305 m	800 m	E-W	U.S. Geological Survey (1981)
Salton Sea	1981	305 m	800 m	E-W	U.S. Geological Survey (1983)
Palen	1955	152 m	400 m	Variable	U.S. Geological Survey (1985)
San Diego	1989	305 m	800 m	N55°E	U.S. Geological Survey (1990)
Twentynine Palms	2002	245 m	530 m	E-W	Sweeney (2002)
San Bernardino Mts	2002	245 m	530 m	N-S	Sweeney (2002)
Joshua Tree	2008	305 m	800 m	N-S	This study

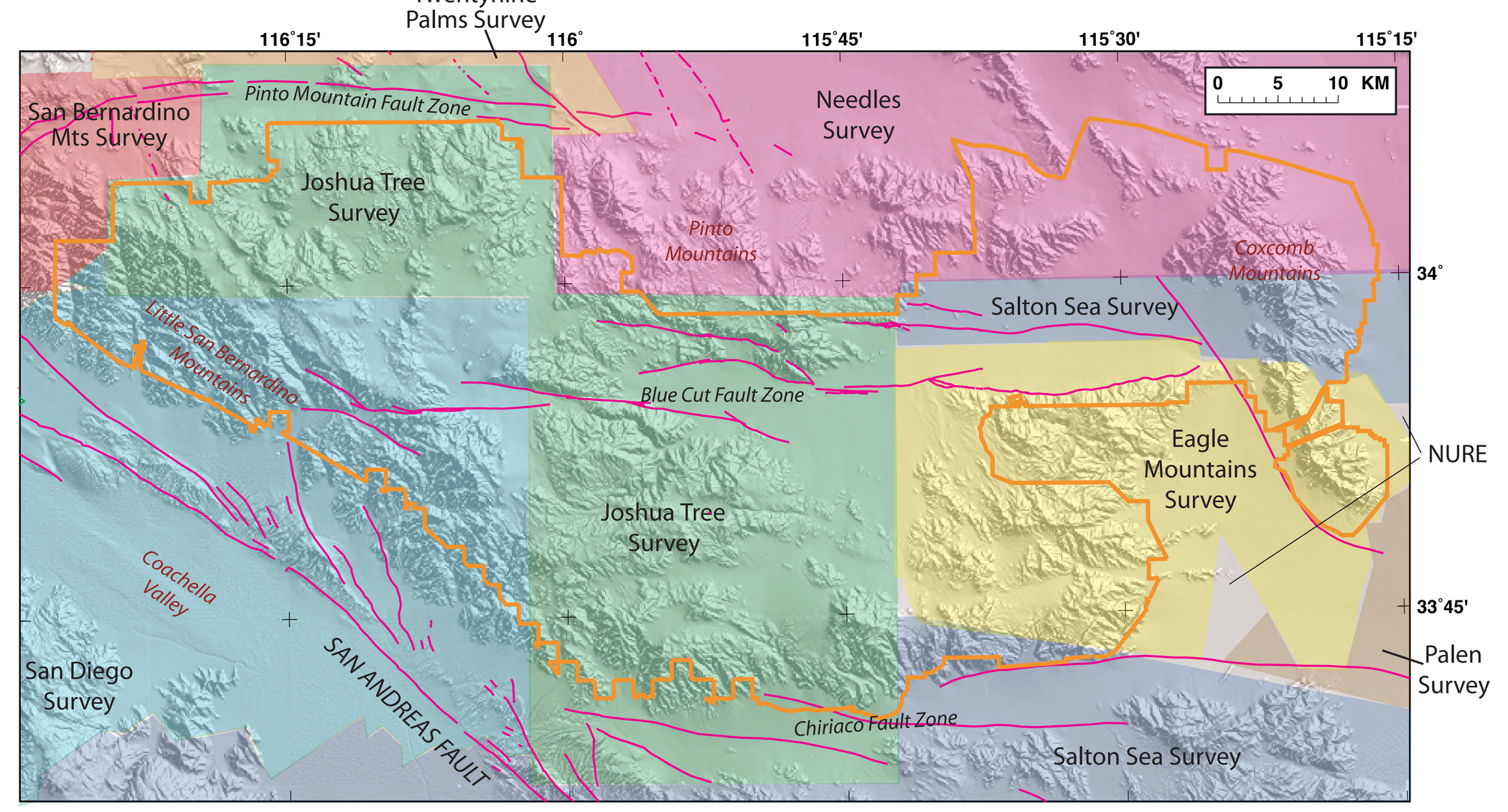
Twentynine Palms Survey
116°15'
116°
115°45'
115°30'
115°15'
0 5 10 KM
San Bernardino Mts Survey
Pinto Mountain Fault Zone
Joshua Tree Survey
Needles Survey
Salton Sea Survey
NURE
Eagle Mountains Survey
Coachella Valley
San Diego Survey
SAN ANDREAS FAULT
Chiriaco Fault Zone
Salton Sea Survey
Palen Survey
34°
33°45'

Figure 1. Shaded-relief topographic map showing major faults (magenta lines; modified from Langenheim and Powell, 2009) and extent of aeromagnetic surveys listed in table 1.

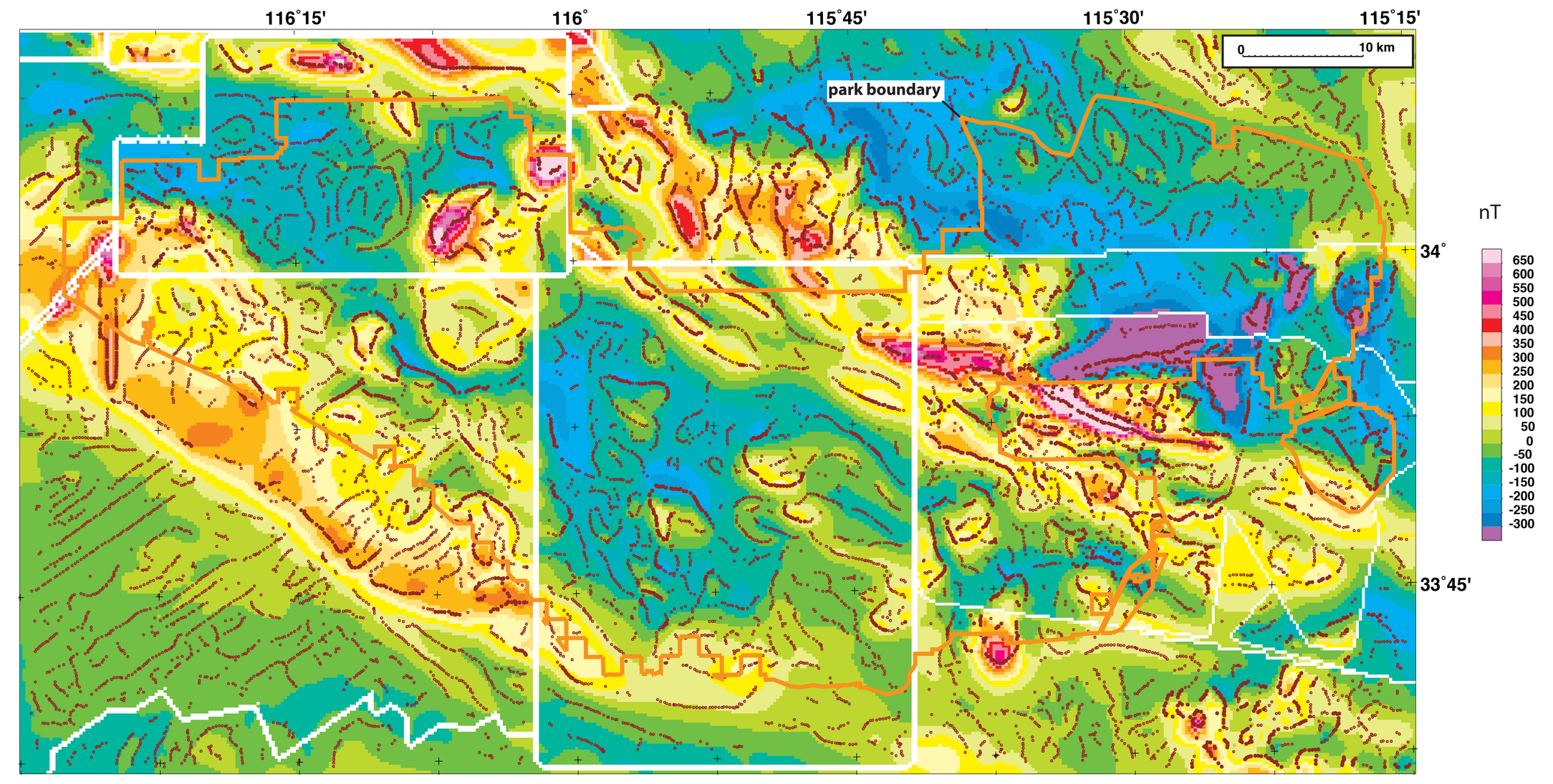

Figure 2. Color-contour aeromagnetic map with magnetization boundaries shown in brown, survey boundaries shown in white.

Available at http://pubs.usgs.gov/of/2010/1070